

Finite Element Modelling of Heat and Moisture Transfer through Cross Laminated Timber Panels

Jaya Tripathi and Robert W. Rice *

The primary objective of this research was to assess and to model the hygrothermal properties of CLT panels made from three distinct combinations of spruce lumber and laminated strand lumber (LSL). The hygrothermal performance of these materials both individually and in conjunction in CLT has not been investigated before and is an important indicator of CLT building wall performance. CLT panels consisting of spruce as a face layer absorbed moisture more rapidly when that face layer was exposed to higher moisture concentration compared to CLT panels consisting of LSL as a face layer. The accumulation of moisture between layers increased with placement of the LSL as a core layer. Based on the smaller diffusion coefficient, moisture transport through the CLT panels made of LSL was slower. Modelling with a finite element-based program showed that the temperature in the panels when exposed to a severe gradient equilibrated within two days, as shown by both experimental and simulated results. For moisture transfer, the diffusion coefficient variation with moisture content and temperature based on the Arrhenius equation produced simulation results in agreement with experimental results but the moisture transfer was much slower than the heat transfer.

Keywords: Hybrid Cross laminated timber; Finite element modelling; Hygrothermal

Contact information: School of Forest Resources, University of Maine, Orono, ME USA 04469;

** Corresponding author: RWRice@Maine.edu*

INTRODUCTION

Cross-laminated timber (CLT) is defined as a prefabricated engineered wood product made of at least three orthogonally bonded lumber layers. Softwoods are usually used for CLT manufacture in North America (Karacabeyli and Douglas 2013). The purpose of this research was to measure both heat and mass transfer through conventional and hybrid CLT panels and to compare the measured data with predictions made using a commercially available finite element modeling program. The mechanical properties and construction techniques of CLT panels have been evaluated extensively, and some hygrothermal data have been reported for CLT panels, but no data exist for the hybrid panel types reported here. Further, given that moisture intrusion is inevitable in wall systems, there is reason to be particularly interested in the potential for moisture accumulation within the panels and whether it could be modeled. Analysis through heat and moisture transfer model will help to prevent issues with buildings in climates that are usually hot or cold and wherever moisture accumulation within wall systems could compromise building integrity. Rapid moisture gain and temperature change are detrimental for energy efficiency and long term durability with respect to moisture related problems.

In addition to using softwoods of the SPF group, an effort was made to incorporate an engineered wood known as laminated strand lumber (LSL) into the CLT panels creating what is termed a hybrid CLT panel. The physical and mechanical properties of the hybrid CLT panels made with this combination of laminae have not been previously assessed and is a new concept. As an engineered product, LSL is uniform, readily available, and easy to work with. Information gained from testing these hybrid CLT panels can help in decision making regarding this new approach to the selection of materials for CLT, which can also affect the value and market potential for these materials. The hygrothermal performance of LSL has not been reported previously, and the combination of LSL and SPF incorporated into CLT panels is also unique. The research also allowed an analysis of the potential for condensation for select CLT configurations. In addition, testing allowed the evaluation of the benefits of using structural composite lumber in CLT panels. Although there are a number of studies related to the strength or moisture related properties of panels (Bayatkashkoli and Faegh 2014; Wang *et al.* 2015; Davids *et al.* 2017), nothing has been reported about the hybrid panels tested here and compared with traditional SPF panels. Moisture performance is a key consideration in wall design (Glass 2013). In a wall assembly, heat and moisture face various resistances to their flow when they pass from one layer to another and proper consideration should be given to the placement of various layers in such a way that risk of moisture damage, which results from prolonged moisture accumulation, is minimized. The balance between entry and removal, which results in least accumulation of moisture, is the key in many assemblies (Lstiburek 2004).

The finite element modeling program (FEM) was produced by COMSOL Multiphysics® (Burlington, MA, USA) and allowed both heat and mass transport to be determined. The intent here is not to examine the workings of the model, but, rather, to apply the model using measured data and compare the predicted results with actual measurements.

The heat transfer in solids section of the FEM uses Fourier's law of heat conduction as the mathematical model for heat transfer in solids (Comsol Multiphysics 2012), as shown in Eq.1,

$$\rho C_p \frac{\partial T}{\partial t} - \nabla \cdot (k \nabla T) = Q \quad (1)$$

where ρ is the density (kg / m³), C_p is the heat capacity (J / (kg - °K)), and k is the thermal conductivity (W / (m - °K)). The discretization for temperature was quadratic.

Moisture transfer through a material using the FEM is accomplished by using a chemical "species" transport module, which in this case is water vapor. The FEM assumes that transport is through ordinary diffusion and convection for mass transfer. In the present case convection internal to the CLT was not applicable, and the governing equation for mass transfer is shown in Eq. 2 (Comsol Multiphysics 2012),

$$\frac{\partial c}{\partial t} = \nabla \cdot (D \nabla c) \quad (2)$$

where c is the the concentration (mol / m³), D is the diffusion coefficient (m² / s), and t is the time (s). The discretization for concentration was linear.

Siau (1984), citing Stamm (1964), stated that the diffusion coefficient increases rapidly with temperature in accordance with the Arrhenius equation as shown in Eq. 3,

$$D_T = C \exp\left(-\frac{E}{RT}\right) \quad (3)$$

where D_T is the diffusion coefficient of wood (cm^2/s), C is the constant, E is the activation energy (cal/mol), and R is the universal gas constant ($1.987 \text{ cal}/\text{mol}/^\circ\text{K}$).

Assuming that Eq. 3 applies, the rate of diffusion would be greater on the warm side of the panel than on the cold side of the panel. According to Siau (1984) the activation energy needed for Eq. 3 can be calculated using Eq. 4,

$$E = 9200 - 70MC \quad (4)$$

where MC is the moisture content of wood in % (dry basis).

In the past, simulation software such as WUFI (Oak Ridge National Laboratory/Fraunhofer Institute of Building Physics) and ABAQUS (Dassault Systèmes, Johnston, RI, USA) have been used to analyze moisture related performance of CLT panels. Lepage (2012) measured the rate of water uptake (via capillary process) of CLT panels, made of some common softwood species, to determine an absorption coefficient “A-value”, which was used later with WUFI software to simulate response of typical CLT wall assemblies when exposed to various climatic conditions likely to be encountered across Canada. Elevated moisture contents were used as the metric of comparison between various CLT wall assemblies. The major conclusion drawn was that CLT panels can be durable (decay resistant) in wall systems for Canadian buildings because very little moisture change occurred throughout the year once equilibrium was reached in the CLT. The panels started at 12% MC. However, Lepage noted that risks associated with degradation can be augmented if moisture is not considered. He emphasized that, depending upon the climate, the ability of the wall to lose moisture, called the drying capacity of the wall assembly, becomes vital for the decay resistance of the CLT panels. From his simulation, it was found that the use of vapor-impermeable membranes on the exterior or the interior of the assembly increases the risk of moisture damage if installed on a wet CLT panel. Lepage also modeled the effects of different kinds of vapor barriers applied to wet CLT assemblies but did not do any field tests. McClung *et al.* (2014) conducted a field level test to assess whether wetted CLT panels are capable of drying within a reasonable time period so that there is no risk of decay and how the wall assembly configurations (permeance of the assembly) influenced the drying of CLT panels. Then they compared that field test’s results with the results of WUFI, to evaluate if simulation program is able to predict such hygrothermal performance accurately. They first wetted CLT panels made from common softwood species in a swimming pool to achieve moisture content (MC) close to or over 30% of MC. After removal from the pool, thermistors and RH sensors were also installed across the wall assemblies to monitor the hygrothermal behavior of the CLT panels. The MC of these CLT wall assemblies was monitored over a one-year period. The field test data were analyzed to evaluate the drying of the tested wall assemblies and compared to hygrothermal simulation results to assess the accuracy of modelling and identify potential areas for improvement. The field data indicated that there were slight differences among wood species but the drying performance of a CLT wall assembly was markedly influenced by the wall design (type of insulation and vapor barriers used). The data showed that none of the CLT walls would likely remain at a high MC level long enough to initiate decay under the conditions tested because most of the CLT panels dried to below 26% within one month except for the CLT walls sections with a low-permeance interior membrane (26% MC, at 20 °C temperature was considered as the benchmark for comparison to determine safety against decay). Low-permeance materials such as polyethylene and non-vapor permeable WRBs caused slower drying of wetted CLTs, and caution was recommended

for their use in case of panels with incidental moisture. Simulation results were generally in good agreement with field measurements at MCs below 26% with adjusted material properties and properly assigned initial conditions.

Gereke (2009) simulated the moisture distribution in CLT consisting of spruce as face layers and medium density fiberboard (MDF) as core layer, using a finite element program called ABAQUS. Because of lower diffusion coefficient of MDF, the bottom layer had more moisture because of water accumulation at the boundary and the top layer remained drier in spruce- MDF laminates compared to panels consisting of three layers of spruce. Häglund (2007) used the finite element program COMSOL and average daily moisture concentration data from across Sweden to model moisture content variation in wood under varying moisture concentration conditions. The model was validated using measured glulam beam data from Jönsson (2004). Inputs for the model included moisture concentration relationships for relative humidity and Kirchoff potential that were determined for small spruce samples and modified during the validation. They concluded that the annual moisture content variation in glulam beams in Sweden probably varied about 6 to 9%. Also, of interest is that the variation in relative humidity, due to weather variations, was quickly dampened by the wood resulting in an average moisture potential within the beams that changed only due to long term surface condition changes.

Finally, Wang and Ge (2016) evaluated the wetting and drying performance of CLT wall assemblies made from five species native to Canada (spruce, SPF, hem/fir). They applied water and wind resistant barriers along with cladding or sheathing on the exterior and interior sides of the assemblies. The measured heat and mass transfer were then modeled using DELPHIN software, version 5.8.3 (Institute for Building Climatology at Dresden University of Technology, Dresden, Germany). The 0.6 m by 0.6 m CLT systems were monitored over a two-year period under the exterior climatic conditions of Waterloo, Ontario, while the interior was maintained at about 21 °C and 50% RH. The results showed that the CLT wall assemblies with low vapor permeance material placed on the exterior side of CLT panel have a higher risk of moisture problem than CLT wall assembly with high vapor permeance material placed on the exterior side of the CLT panel. The moisture diffusivity was determined based on the laboratory water uptake tests, but unlike the software program used here and in Häglund (2007), the Delphin program uses liquid conductivity to model moisture transport, which is not likely to occur with the panels. The goal of this research was to provide an analysis of the potential for condensation in three CLT configurations and to use measured data to evaluate the prediction of a hygrothermal model. The detailed measurements also were used to recommend approaches that can more closely align the hygrothermal simulation with actual measured data. The scope of the research is to observe the trend of heat and moisture transfer and does not go beyond that, such as for analysis of moisture-induced stress.

EXPERIMENTAL

CLT Panel Types and Preparation

To corroborate the results from the simulation and obtain input data for the simulation, a series of experiments were conducted using CLT panels with three different compositions. The first panel type consisted of three layers of Eastern red spruce (*Picea rubens*); the second panel consisted of red spruce face layers and LSL in the core layer;

and the third panel consisted of LSL face layers and a red spruce core layer. Two panels of each composition were tested, and the data were averaged. The lumber was obtained from a mill in Dover-Foxcroft, ME and the LSL, graded 1.35E, was obtained from Louisiana-Pacific Corporation in Houlton, ME. To manufacture the panels, spruce and LSL “boards” were cut to appropriate size. For the face layers of a panel, they were about 90 cm long by 15 cm wide by 3.8 cm thick. For each panel face, the four boards comprising the laminae were selected to have minimal defects. For the core layers, six boards were cut to a size of approximately 60 cm long by 15 cm wide by 3.8 cm thick. Four boards were selected for face layers and six boards were selected for core layers to get a CLT panel of approximately 90 cm by 60 cm. Boards of the core layer were oriented orthogonally with respect to boards of face layers. Each board was planed before applying adhesive, and after planing the thickness of each board in the laminae measured about 3.5 cm. Within two hours of planing, PURBOND HB E452, a polyurethane adhesive (Henkel Corporation, Rocky Hill, CT) was applied to the laminae at a target spread rate of 146 g / m² and the panel was cold-pressed at about 1034 kilopascal for 2 hours. To prevent lateral movement during layup and pressing, the boards were clamped laterally to reduce gaps between the boards as much as possible and were also held in place as layer with help of wood strips and screws at the edges.

CLT Panel Monitoring and Environmental Control

Two three layered CLT panels, each measuring approximately 90 cm high by 60 cm wide were tested simultaneously by using them as two walls in a small chamber within a larger incubator type chamber (Fig. 1). Within the small insulated chamber, the temperature and relative humidity was controlled. The temperature-controlled incubator/environmental chamber was kept at a low temperature (~4 °C) for the duration of the experiments. The plan was to keep the interior of the chamber warm and moist and the exterior cool and dry, as illustrated in Fig. 1. Using this configuration, and after equilibration, thermal energy and moisture would flow from the interior of the chamber towards the exterior of the panels. The conditions chosen for the interior and exterior were not based on weather data but were severe and would clearly show moisture accumulation potential and heat transfer through the panels. Inside each panel, two sensors were located at each glue line. The sensor at the bottom position was beyond a glue line. Two temperature/RH sensors measuring 10 x 35 mm (Model: S-THB-M008, Onset Company, Bourne, MA) were inserted into the panels to monitor temperature and relative humidity as shown in Fig. 1. These sensors were connected to a HOBO U30 monitoring station (Onset Company, Bourne, MA) and, in turn, connected to Hoboware software (Onset Company, Bourne, MA), which was used for launching, reading out, and plotting data from HOBO data loggers.

A 900-watt, 30.5 cm long finned strip heater was placed midway between two panels to make that side of panel warm (Fig. 2) and controlled using an Omega Engineering (Norwalk, CT) temperature controller (model CN732). The target temperature within the small chamber was 29 °C.

To obtain a high relative humidity in the small chamber, an ultrasonic humidifier (Model MIST-PAC 5, Humidifirst, Inc., Boynton Beach, FL, USA) was used to generate humidity. The humidifier controller (model TCY-BH-TU-W04, Vector Controls GmbH, Wetzikon, Switzerland), also provided by Humidifirst Inc., was connected to a humidity sensor (Model: SDC-H1-16-A2-1, Vector Controls GmbH, Wetzikon, Switzerland), to

maintain the target humidity of 85%. Additional data loggers (Fig. 2) (Model: UX100-003, Onset Company, Bourne, MA) were attached inside the test chamber and on a wall of the incubator to record temperature and relative humidity throughout the test period at respective locations, which were also read out using Hoboware software. All the edges were sealed and insulated. Both the outside and inside conditions were intended to be constant throughout the test period with the above described system; however, it was necessary to keep track and monitor these conditions with the help of these sensors, and the average data were used in the final analysis. The model required that moisture conditions be entered as concentrations in mol/m^3 . So, the temperature and relative humidity values at the boundaries were converted to mol/m^3 using the ideal gas equation.

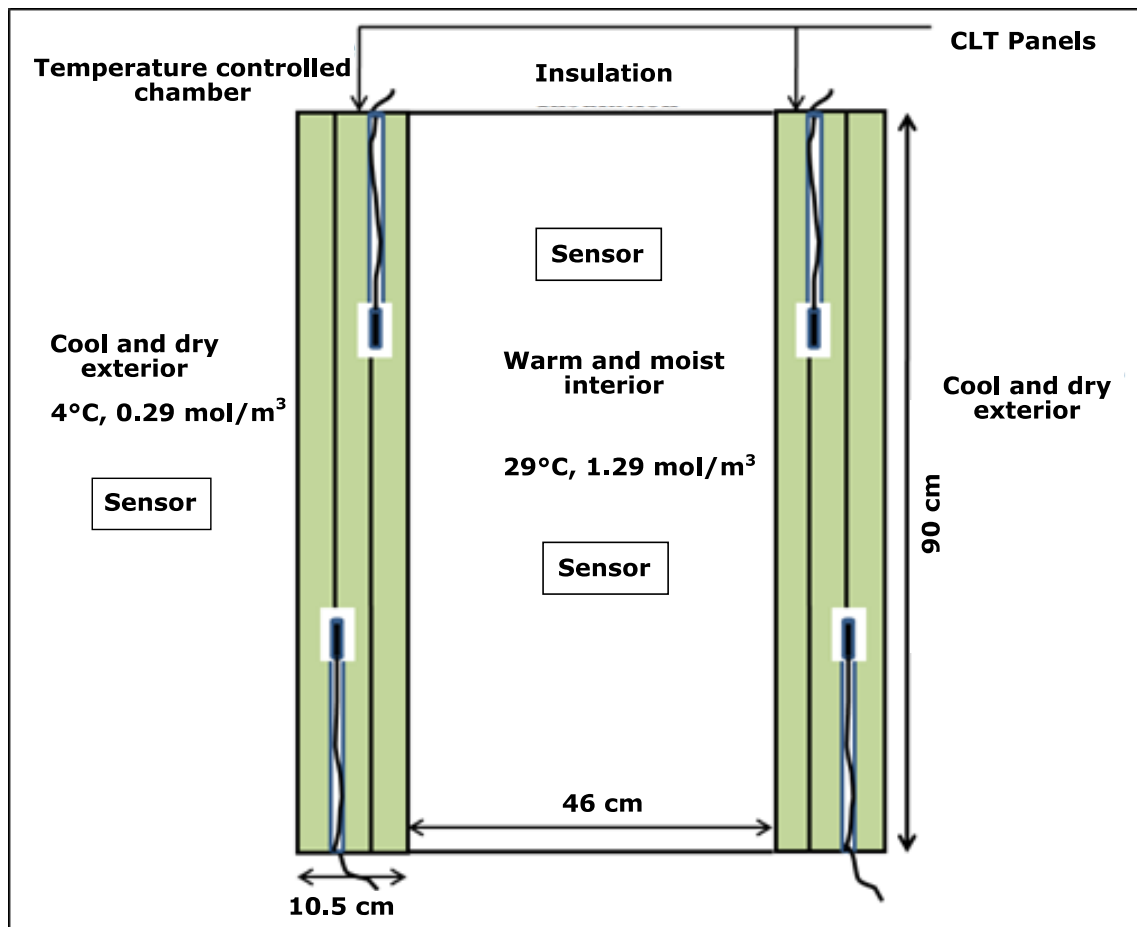


Fig. 1. Experimental approach for panel testing; front view showing approximate environmental conditions and placement of sensors inside the panels; panel edges shown

The entire apparatus was placed in a temperature-controlled incubator/environmental chamber (Fig. 2) and kept at approximately 4 °C for the duration of the experiments. Although the relative humidity could not be controlled, the humidity within the chamber was relatively constant, as described below. Once started, measurements were continuous and lasted a minimum of 30 days. The longest test was 90 days.

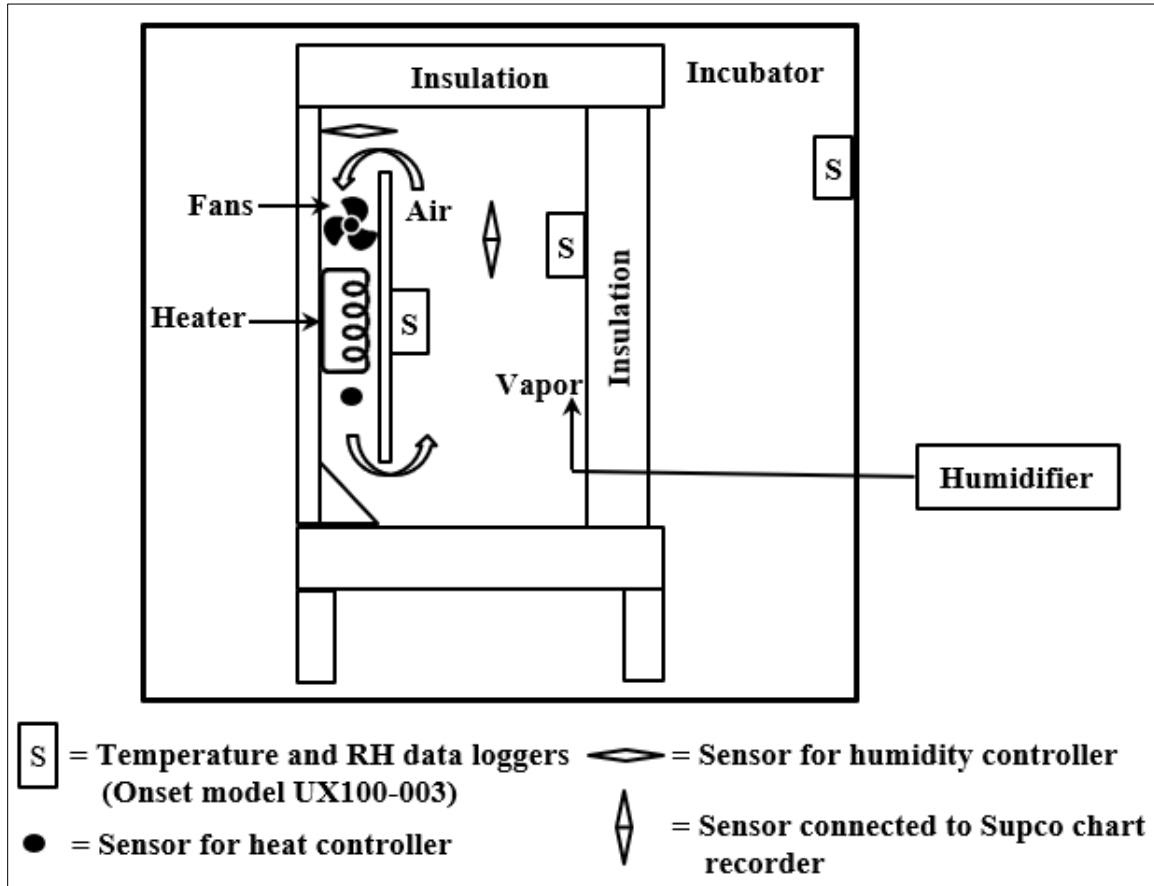


Fig. 2. Details showing the location of equipment inside chamber; this side view shows how the system was constructed

FEM Modelling of Heat and Moisture Transfer through CLT Panels

The model used was a general purpose multi-faceted software program for modelling various physical phenomena. The model for one dimensional heat and moisture transfer through CLT panels was used with either measured or calculated boundary and initial conditions from our experiments. For the full-sized panel measurements, the panels typically measured 10.5 cm thick by 90 cm long by 60 cm deep (Fig. 1). Sensor channels, 23 cm deep by 0.5 cm wide, were followed by chambers of 2 cm wide and 5 cm long for the RH/temperature sensor. These are drawn at their respective locations in Fig. 1. For modeling, the panels were assigned the boundary conditions calculated from measured temperature and relative humidity conditions that were averaged and are shown in Table 1. The initial temperature of the panels was about 293 K (20 °C).

Table 1. Boundary Conditions Used in Modelling (From Experimental Data)

Interior Boundary temp. (Kelvin)	Exterior Boundary temp. (Kelvin)	Interior Boundary Conc. (mol / m ³)	Exterior Boundary Conc. (mol / m ³)	Initial Temperature (Kelvin)
302.6 (29.5 °C)	277.4 (4.25 °C)	1.29	0.29	293.15 (29 °C)

Modeling of heat transfer through CLT panels

Table 2 summarizes the values of different parameters related to heat transfer that were assigned to each layer. The values for LSL and spruce in the Table 2 were derived from the data collected, except for specific heat capacity values. Equations for specific heat capacity of OSB and for solid wood given by Rice and Redfern (2016) were used for approximate calculations of specific heat capacity of LSL and of spruce, respectively. A detailed explanation of determination of thermal conductivity values is described by Tripathi and Rice (2017). No separate thermal conductivity value was assigned for the glue line because of its non-significant thickness in comparison to total thickness.

Table 2. Heat Transfer Parameter Values for the FEM

Parameters	Spruce	LSL
Thermal conductivity (12% MC), (W / m - K)	0.105	0.115
Density (kg / m ³)	470	700
Specific heat capacity (20 °C and 12% MC) (joules / kg - K)	1591	1465

Input data for modeling moisture transport through CLT panels

The diffusion coefficient values (D_T) of LSL and spruce were measured using a slightly modified wet-cup method, as described in ASTM E96 (ASTM 2005). The average diffusion coefficient of LSL was $5E-11$ m²/s at room conditions, which was about 22 times smaller than that of spruce, which averaged $2.24E-10$ m²/s. The lower diffusion coefficient value of LSL can be attributed to its high density. Also, LSL is a composite product that contains adhesive. Steam injection pressing and densifying reduced D_T when compared to spruce.

A temperature gradient existed across the panels during the testing. To incorporate the temperature effect on diffusion the Arrhenius equation was used (Eq. 3). The constant C was calculated for spruce and LSL using the diffusion coefficient values calculated at room temperature (D_T). The results used for modeling are shown in Table 3.

Table 3. Determination of the Constant "C" from Calculated Diffusion Coefficient Values

	D_T (m ² /s)	MC (%)	Temperature (K)	Activation Energy* (cal / mol)	RT^* (cal / mol)	C (m ² /s)
Spruce	2.24×10^{-10}	12	298	-8360	592.126	3×10^{-04}
LSL	5.00×10^{-11}	12	298	-8360	592.126	7×10^{-05}

*Activation energy calculated as $E = 9200 - 70MC$; $R = 1.987$ cal / K / mol

Because the activation energy depends on moisture content, the activation energy for each layer was calculated from the interior side towards the exterior (Eq. 4). The values were 8150 cal/mol, 8430 cal/mol, and 8570 cal/mol at 15%, 11%, and 9% MC, respectively. The moisture content values were based on post-test measurements of panel layer MC. Using the activation energy for each layer and the calculated value of " C ", the Arrhenius type equations shown in Table 4 were used to calculate how the diffusion coefficient values (m²/s) changed with panel temperatures and those values were used in the FEM.

Table 4. Diffusion Coefficient Equations Used for Spruce and LSL Based on the Arrhenius Equation

Layer	Spruce	LSL
1st	$3E-4\exp(-8150/1.987T)$	$7E-5\exp(-8150/1.987T)$
2nd	$3E-4\exp(-8430/1.987T)$	$7E-5\exp(-8430/1.987T)$
3rd	$3E-4\exp(-8570/1.987T)$	$7E-5\exp(-8570/1.987T)$

The diffusion coefficient for air (Engineering ToolBox 2005) of $22 \times 10^{-06} \text{ m}^2/\text{s}$ was used for the air within the interior sensor chambers. Finally, to calculate a vapor barrier effect, Gereke's (2009) approximation was used. It was assumed that the diffusion coefficient of the polyurethane within 0.1 mm thick glue lines would be 500 times less than that of spruce, *i.e.*, $4 \times 10^{-13} \text{ m}^2/\text{s}$. The panels were at about 7% EMC before testing, and the initial relative humidity was about 35% at the sensor locations within the panels at 20 °C. Using those conditions, the moisture concentration was approximately $0.3 \text{ mol}/\text{m}^3$, which was considered to be the initial condition for modeling purposes.

RESULTS AND DISCUSSION

Using the values given in Tables 1 and 2, the temperature was modeled and compared with actual measured date. The time series results are shown in Fig. 3.

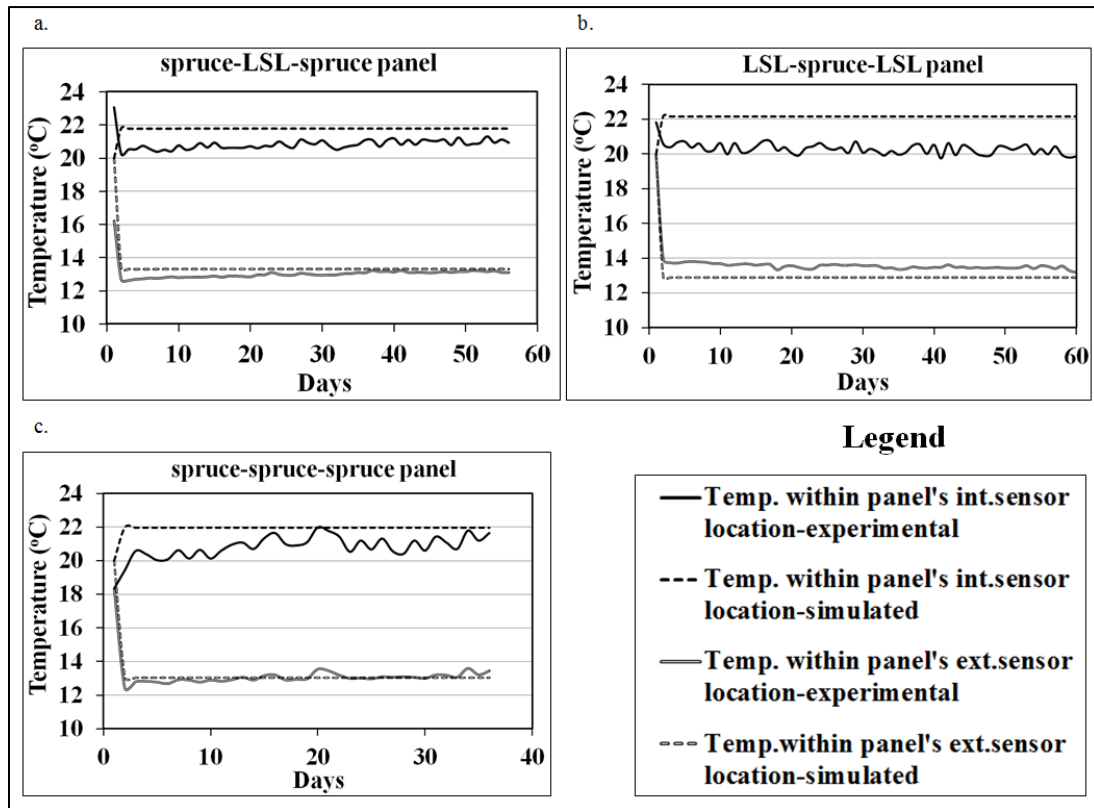


Fig. 3. Experimental vs. simulated temperatures within CLT panels; a = spruce-LSL-spruce panels, b = LSL-spruce-LSL panels, and c = spruce-spruce-spruce panels; only one replicate of each CLT type is shown for clarity (int. = interior, ext. = exterior). The data for both replicates were similar.

It was clear that the simulated and measured time-series temperature profiles were well matched, particularly for the sensors located toward the exterior of the panels. To quantify the variation, the maximum deviations between experimental and simulated values for the different panel types are shown in Table 5. A maximum deviation between the experiment and the simulation of below 7% for all the panels shows that experimental and simulated heat transfer results were in good agreement with each other. The starting point for picking out a maximum deviation value from all the deviation values was the seventh day.

Table 5. Quantification of the Error between Experimental and Simulated Temperatures

Panel	Maximum Deviation at Panel's Interior Sensor Location	Maximum Deviation at Panel's Exterior Sensor Location
spruce-LSL-spruce	4%	2%
LSL-spruce-LSL	6%	3%
spruce-spruce-spruce	5%	2%

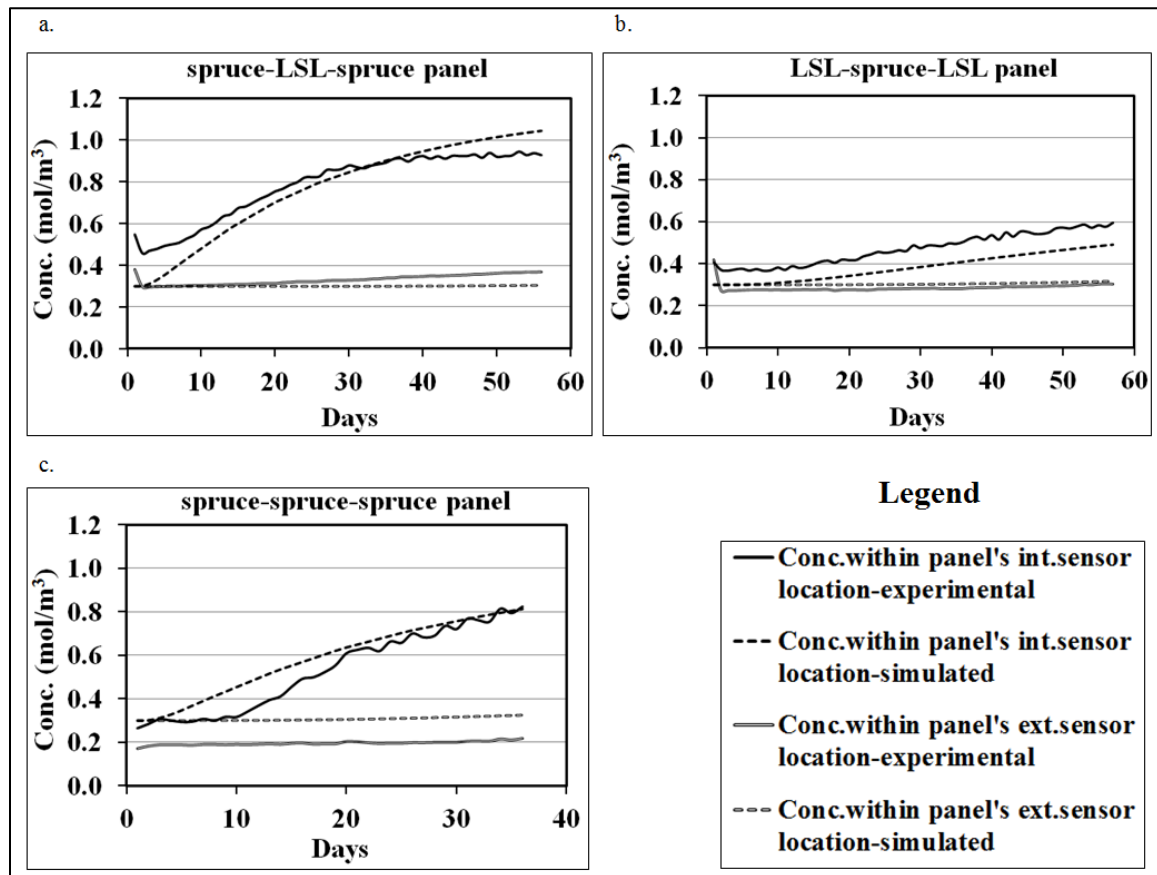


Fig. 4. Comparison of experimental and simulated moisture concentrations (conc.) within CLT panels; a = spruce-LSL-spruce panels, b = LSL-spruce-LSL panels and c = spruce-spruce-spruce panels; only one replicate of each CLT type is shown for clarity. The data for both replicates were similar.

After inserting all the values related to moisture transfer along with the diffusion coefficient expressions (Table 4), moisture transfer was simulated, and the resulting concentrations at sensor locations over a period of time were compared with the experimental results shown in Fig. 4. As shown, the trend of the simulated results matched well with the experimental results. Both the measured data and the simulation showed that, at the inside sensor locations, the moisture concentration was highest in the spruce-LSL-spruce panel, and lowest in the LSL-spruce-LSL panel. The increase in moisture concentration of the spruce-spruce-spruce panels were between those of the other panel types. The increase in moisture concentration in the spruce-spruce-spruce panels was slightly lower than that of spruce-LSL-spruce panels but much higher than that of LSL-spruce-LSL panels.

Issues with Initial Concentration

The FEM requires that an initial moisture concentration within the panel be entered into the program, and using the assumed value of $0.3 \text{ mol} / \text{m}^3$ created a small problem at the beginning of the modeling time period. The problem occurred because the initial moisture concentration of the entire warm and dry panel on day one was not really representative of the conditions within the panel after a brief period of exposure to the warm/moist chamber interior and the cool/dry chamber exterior. Also, while the temperatures within the panel interior quickly stabilized, the moisture concentrations within the panel sensor locations were influenced by the exterior conditions only after an extended period of exposure. After analysis, it was decided to adjust the panel initial moisture concentrations to the temperature and relative humidity as measured by the sensors within the panels after temperature stabilization. Table 6 shows the values of initial measured moisture concentrations calculated from the experimental data on day two of testing. Making the adjustments created different initial concentrations at the interior and exterior panel sensor locations, for the same panel. For example, the initial concentration was $0.37 \text{ mol} / \text{m}^3$ inside the panel's interior sensor location and $0.3 \text{ mol} / \text{m}^3$ inside the panel's exterior sensor location for LSL-spruce-LSL panel (Table 6).

Different panel types had slightly different initial moisture concentration values at the same interior sensor locations. For example, for the LSL-spruce-LSL panel the moisture concentration was $0.37 \text{ mol}/\text{m}^3$, and the spruce-spruce-spruce was $0.3 \text{ mol}/\text{m}^3$ at the panel's interior sensor location nearest the warm/moist chamber. This could be because these panels were tested at different times of the year and the absolute humidity or concentration of water vapor, which is a function of relative humidity and temperature, might also be different at different times of the year due to varying ambient temperature and humidity conditions.

Table 6. Initial Moisture Concentration of Panels as Calculated from the Experiments (Data are from the Sensors within the Panels)

Panel	Initial Moisture Concentration for Interior Sensor Location (mol/m^3)	Initial Moisture Concentration for Exterior Sensor Location (mol/m^3)
Spruce-LSL-spruce	0.46	0.30
LSL-spruce-LSL	0/37	0.30
Spruce-spruce-spruce	0.30	0.17

The assumed initial moisture concentration, without adjustment, was $0.3 \text{ mol} / \text{m}^3$, but some of the adjusted values shown in Table 6 differed and were adjusted to the calculated values for modeling. Comparing Figs. 4 and 5 shows that this manner of adjusting the initial moisture concentration values would help to obtain simulated results close to experimental results. One exception was Fig. 5a, where the deviation between experimental and simulated values diverged at the panel's interior sensor location of spruce-LSL-spruce. The divergence is likely the result of sensor inaccuracy at very high relative humidity values. The maximum deviations between experimental and simulated values after adjustment for the different panels are shown in Table 7. The starting point for picking out a maximum deviation value from all the deviation values was the seventh day. Most of the deviations between the experimental and simulated were much less than shown in Table 7.

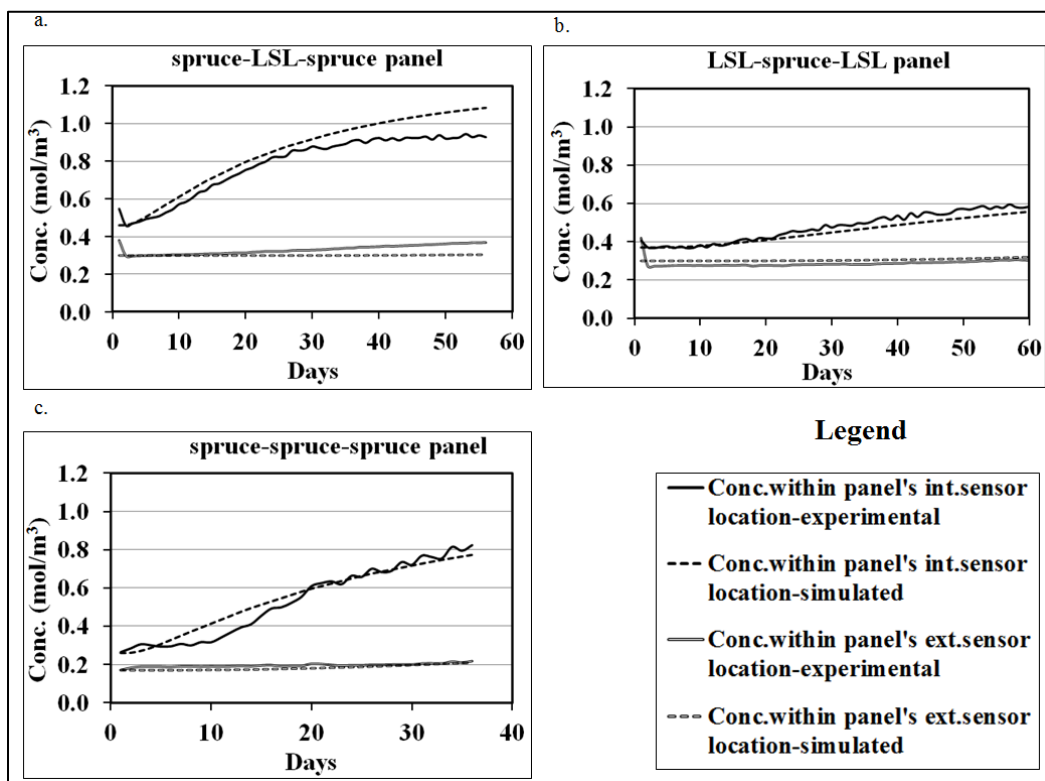


Fig. 5. Comparison of experimental and simulated moisture concentrations within CLT panels after adjusting initial moisture concentration values; a = spruce-LSL-spruce panels, b = LSL-spruce-LSL panels, and c = spruce-spruce-spruce panels; only one replicate of each CLT type is shown for clarity

Because of higher diffusion coefficient values of spruce, CLT panels consisting of spruce as a face layer absorbed moisture more rapidly when that face layer was exposed to higher moisture concentration when compared to CLT panels consisting of LSL as a face layer. The accumulation of moisture between layers increased with placement of the LSL as a core layer. Based on the smaller diffusion coefficient, moisture transport through the CLT panels made of LSL was slower. Among the tested combinations, the potential for moisture damage is lowest in the LSL-spruce-LSL panel and highest in the spruce-LSL-spruce. The non-composite, all-wood spruce-spruce-spruce is intermediate in terms of potential moisture damage. Panels in extreme conditions require moisture barriers which are common practice.

Table 7. Quantification of the Error between Experimental and Simulated Moisture Concentrations after Adjustment of the Initial Moisture Concentration

Panel	Maximum Deviation At panel's Interior Sensor Location	Maximum Deviation At Panel's Exterior Sensor Location
spruce-LSL-spruce	17%	21%
LSL-spruce-LSL	8%	10%
spruce-spruce-spruce	43%	11%

Few, if any, buildings would be subjected to the difficult environmental conditions that were used for this research for a period of 60 days. The present research shows that the panels, unprotected by a vapor barrier, gain moisture quickly. Conversely, the same panels subjected to the common wet/dry cycles lose moisture quickly. The addition of a vapor barrier, as shown in the next section is added protection.

Applying the Finite Element Model

Since the model results closely matched the measured data after some slight adjustments, the program was used to predict what level of protection the panels require to prevent moisture concentrations near the dew point within the panels. As an example, modelling of moisture transfer was done using the panel with the highest potential for the moisture related degradation, which was the spruce-LSL-spruce panel. One layer of polyethylene sheet was added on that face of the panel, which was exposed to warm/moist conditions. Values for the polyethylene sheet that were used for modelling are shown in Table 8.

Table 8. Physical Properties of Polyethylene

Properties	Values
Diffusion coefficient	$7.8 \times 10^{-12} \text{ m}^2 / \text{s}$ (Perry and Snoddy 1996)
Thermal conductivity	$0.33 \text{ W} / \text{m} \cdot \text{K}$ (Professional Plastics 2016)
Density	$940 \text{ kg} / \text{m}^3$ (D&M Plastics Inc. 2016)
Specific heat capacity	$1900 \text{ J} / \text{kg} \cdot \text{K}$ (Professional Plastics 2016)

After adding the polyethylene sheet and using the panel properties, the simulation results shown in Fig. 6 were obtained.

The decrease in the moisture concentration within the panels means reduced the possibility of reaching the dew point condition and the panels would be at less risk of moisture damage. Figure 6 shows that polyethylene sheet of 0.5 mm thickness, and diffusion coefficient value of $7.8 \times 10^{-12} \text{ m}^2 / \text{s}$ will provide fair protection to the panel. However, one can resort to 1 mm thick polyethylene sheet, even if that would be more expensive, to provide better protection to these panels that are under extreme environmental conditions. Also, material less than 0.5 mm thick might provide better protection if it has a lower diffusion coefficient value.

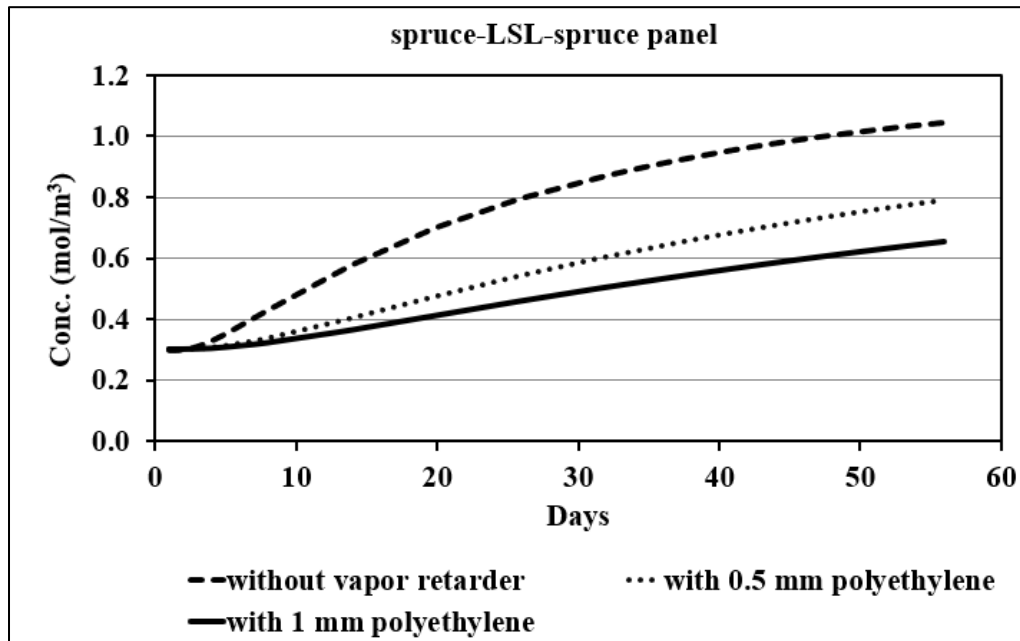


Fig. 6. Effect of reducing the accumulation of moisture at the internal sensor location after adding polyethylene sheet of various thicknesses

Wall design using CLT requires careful analysis of material types and material placement according to boundary conditions (climate) in order to avoid moisture accumulation and eventually moisture damage.

CONCLUSIONS

1. The trends of heat and moisture transfer with time shown by modelling results were close to experimental results.
2. Heat transfer modelling also showed that heat transfer equilibrates quickly, in two days, and remains steady. Maximum differences between experimental and simulated results were below 7% for all panels.
3. Moisture transfer modelling results were close to experimental results after the diffusion coefficient values were adjusted to changing temperature and activation energy values in accordance with the Arrhenius equation. At sensor locations, within the panels, moisture concentration was highest in spruce-LSL-spruce panel, and lowest in LSL-spruce-LSL panel.
4. The rate of moisture accumulation during testing in the spruce-spruce-spruce panels was slightly lower than that of the spruce-LSL-spruce panels but much higher than that of LSL-spruce-LSL panels. The simulation and experimental results closely aligned.
5. A limitation with the particular FEM that was used was the inability to parameterize and functionalize the moisture content of wood. The model used is a general simulation software package, not specifically designed for wood, and the accuracy of the modeled results will depend on the accuracy of the assumed moisture content values.

6. The FEM can be used to determine the type and thickness of vapor retarder should be used under typical environmental conditions.

ACKNOWLEDGEMENTS

The authors gratefully acknowledge the support of the Agriculture and Food Research Initiative Special Research Grants Program – Competitive Grant No. 2013-34638-21491 from the National Institute of Food and Agriculture, U.S. Department of Agriculture and the USDA McIntyre Stennis program project ME041712. The authors would also like to acknowledge the Northeast Lumber Manufacturers Association (NeLMA), LP Building Products, Pleasant River Lumber Company, and the Henkel Corporation for providing materials used in the study. This is MAFES report #3536.

REFERENCES CITED

- ASTM. (2005). “ASTM E96/E96M: Standard test methods for water vapor transmission of materials,” West Conshohocken, PA.
- Bayatkashkoli, A., and Faegh, M. (2014). “Evaluation of mechanical properties of laminated strand lumber and oriented strand lumber made from Poplar wood (*Populus deltoides*) and Paulownia (*Paulownia fortunei*) with urea formaldehyde adhesive containing nanoclay,” *International Wood Products Journal* 5, 192-195. DOI: 10.1179/2042645314Y.0000000064
- Comsol Multiphysics (2012). *Comsol Multiphysics User’s Guide*, (<http://people.ee.ethz.ch/~fieldcom/pps-comsol/documents/User%20Guide/COMSOLMultiphysicsUsersGuide.pdf>), Accessed on February 7, 2016.
- D&M Plastics Inc. (2016). “Polyethylene,” (<http://www.plasticmoulding.ca/polymers/polyethylene.htm>), Accessed on September 26, 2016.
- Engineering ToolBox. (2005). “Diffusion coefficients of gases in excess of air,” (https://www.engineeringtoolbox.com/air-diffusion-coefficient-gas-mixture-temperature-d_2010.html), Accessed on March 16, 2016.
- Gereke, T. (2009). *Moisture-induced Stresses in Cross-laminated Wood Panels*, Ph.D. Dissertation, ETH Zurich, Zurich, Switzerland.
- Glass, S. V. (2013). *Hygrothermal Analysis of Wood-frame Wall Assemblies in a Mixed-humid Climate* (Research Paper FPL-RP-675), U. S. Department of Agriculture, Forest Products Laboratory, Madison, WI.
- Häglund, M. (2007). “Moisture content penetration in wood elements under varying boundary conditions,” *Wood Science and Technology* 41(6), 477. DOI: 10.1007/s00226-007-0131-z
- Jönsson, J. (2004). “Internal stresses in the cross-grain direction in glulam induced by climate variations,” *Holzforschung* 58(2), 154-159. DOI: 10.1515/HF.2004.023
- Karacabeyli, E., and Douglas, B. (2013). *CLT Handbook*, FP Innovations, Quebec, Canada.
- Lepage, B. R. T. M. (2012). *Moisture Response of Wall Assemblies of Cross-Laminated Timber Construction in Cold Canadian Climates*, MS Thesis, University of Waterloo,

Ontario, Canada.

- Lstiburek, J. (2004). *Vapor Barriers and Wall Design* (Research Report-0410), Building Science Press, Westford, MA, USA.
- McClung, R., Ge, H., Straube, J., and Wang, J. (2014). "Hygrothermal performance of cross-laminated timber wall assemblies with built-in moisture: Field measurements and simulations," *Building and Environment* 71, 95-110. DOI: 10.1016/j.buildenv.2013.09.008
- Perry, R. B., and Snoddy, R. (1996). *Method for Testing the Diffusion Coefficient of Polymer Films*, U.S. Environmental Protection Agency, National Risk Management Research Laboratory, Research Triangle Park, NC, USA.
- Professional Plastics (2016). "Thermal properties of plastic materials," (<http://www.professionalplastics.com/professionalplastics/ThermalPropertiesofPlasticMaterials.pdf>), Accessed on September 26, 2016.
- Rice, R. W., and Redfern, I. (2016). "Heat capacity and its variation with moisture content for plywood and oriented strandboard sheathing produced by North American mills," *Forest Products Journal* 66(7/8), 143-148.
- Siau, J. F. (1984). *Transport Processes in Wood*, T. E. Timell (ed.), Springer-Verlag, Heidelberg, Germany, pp. 245.
- Tripathi, J., and Rice, R. W. (2017). "Thermal conductivity values for laminated strand lumber and spruce for use in hybrid cross-laminated timber panels," *BioResources* 12(4), 8827-8837.
- Wang, L., and Ge, H. (2016). "Hygrothermal performance of cross-laminated timber wall assemblies: A stochastic approach," *Building and Environment* 97, 11-25. DOI: 10.1016/j.buildenv.2015.11.034
- Wang, Z., Gong, M., and Chui, Y. H. (2015). "Mechanical properties of laminated strand lumber and hybrid cross-laminated timber," *Construction and Building Materials* 101, 622-627. DOI: 10.1016/j.conbuildmat.2015.10.035

Article submitted: March 12, 2019; Peer review completed: May 25, 2019; Revised version received and accepted: June 14, 2019; Published: June 19, 2019.

DOI: 10.15376/biores.14.3.6278-6293